JOURNAL OF PROPULSION AND POWER
Vol. 25, No. 4, July–August 2009

Creation of Onset Voltage Hash by Anode Spots in a Magnetoplasmadynamic Thruster

Luke Uribarri* and Edgar Y. Choueiri†
Princeton University, Princeton, New Jersey 08544

DOI: 10.2514/1.40847

Experimental results are presented which quantify the evolution with rising $J^2/\dot{m}$ (ratio of current squared to mass flow rate) of onset voltage fluctuations in a magnetoplasmadynamic thruster operating with three anode materials, and an anode spot model is presented which provides a physical explanation for the properties of these fluctuations. Voltage signals taken in the magnetoplasmadynamic thruster operating below and above onset with anodes of copper, graphite, and lead are analyzed using the statistical measures of probability density and power spectrum. A model of voltage hash as the random superposition of many anode spotting events is used to generate voltage fluctuations with statistics similar to the observed data. The experimental fluctuation statistics evolve with rising $J^2/\dot{m}$ first away from Gaussian, and then back toward Gaussian, with the values of skewness and kurtosis peaking at $J^2/\dot{m} \sim 110\ \mathrm{kA^2 \cdot s/g}$; this behavior is the same for all three anode materials. Nonstationarity in the statistics is shown using high-speed video to be a result of unsteady anode evaporation. The statistics of modeled voltage hash are shown to be functions of the product of the frequency of anode spotting events and their duration, with the statistics becoming more Gaussian as this product grows. Comparison of experimental and model results suggests that, above $J^2/\dot{m} \sim 110\ \mathrm{kA^2 \cdot s/g}$, anode current conduction fragments into an increasing number of anode spots.

Nomenclature

C	=	sheath capacitance
d	=	anode mark size
f	=	frequency
I_e	=	total spot current
J	=	magnetoplasmadynamic thruster total current
k	=	Boltzmann constant
M	=	atomic mass
$\dot{m}$	=	mass flow rate
n	=	spot event occurrence rate
p_{sat}	=	saturation vapor pressure
R	=	spot resistance
T	=	temperature
V	=	voltage
Γ	=	anode erosion rate
τ	=	spot event rise time

I. Introduction

THE magnetoplasmadynamic thruster (MPDT) is a coaxial gas-fed electromagnetic plasma accelerator. Two basic variables of interest control its operation: the current J flowing through the discharge chamber and the mass flow rate $\dot{m}$ of propellant. Improvements in thrust, specific impulse, and thrust efficiency [1] all come with increases in the parameter $J^2/\dot{m}$. However, in pursuing large $J^2/\dot{m}$, whether by raising J or lowering $\dot{m}$, the onset phenomenon is encountered. This is a condition in which the thruster voltage (quiescent at low $J^2/\dot{m}$) fluctuates with an amplitude that can be large compared with the mean voltage and in which the MPDT anode sustains significant damage. Onset is a lifetime-limiting factor in the operation of the MPDT and so must be understood and overcome to improve the performance of MPDTs.

Onset has been a subject of study for several decades. In that time, many observations regarding the critical current above which onset phenomena are likely to appear have been made: in particular, that the critical value of the parameter $J^2/\dot{m}$ can be changed by suitable alterations of the thruster geometry [2–4] or the propellant type [2]. Many theories have been put forth to try to explain the occurrence of onset at the critical value of $J^2/\dot{m}$ [5–7], but the most well-supported theory is that of anode starvation, which states that the thruster will enter onset when the total current exceeds the sheath-limited current-carrying capability of the near-anode plasma [8–11].

What has received less attention is the behavior of the thruster when onset has been exceeded: that is, the behavior of the fluctuating voltage and the damage caused on the anode that are both hallmarks of a thruster operating above onset. As to the latter, Vainberg et al. [12], Hugel [8,13], and Diamant [10] have all observed that anode damage occurs in discrete spots. Kurtz et al. [14] also note the importance of luminous spots that form on the anode concurrently with the initiation of the voltage hash and showed that the onset current can be raised moderately (at best, by 5%) if up to 10% of the propellant is injected near the anode to prevent discharge constriction to spots. Rudolph et al. [15] and Ho [16] have shown that evaporation of anode material occurs at $J^2/\dot{m}$, similar to that at which voltage fluctuations begin. The voltage fluctuations themselves have been correlated with fluctuations in other thruster parameters, such as the optical emission [17], electric and magnetic fields [18], and plasma density [19]. In our previous work [20], we have shown a correlation between voltage hash and the emission of light from anode material in the discharge, though the actual relationship between the two remained unclear.

It is our desire to understand the origin of the voltage fluctuations (hash), so that this knowledge can be applied to the development of ways to circumvent, or to at least delay in $J^2/\dot{m}$, the appearance of the hash and perhaps also the anode damage. For that reason, in this paper, we do not attempt to predict the occurrence of onset; rather, we undertake to present an experimental study of the voltage hash, focused on identifying quantifiable descriptive measures for the evolution of the hash with $J^2/\dot{m}$ and with changing anode material. We calculate the relevant statistics that describe the hash, show that the observed anode damage is consistent with our voltage hash

Presented as Paper 5080 at the 44th AIAA/ASME/SAE/ASEE Joint Propulsion Conference and Exhibit, Hartford, CT, 21–23 July 2008; received 6 September 2008; revision received 3 February 2009; accepted for publication 22 February 2009.

*Currently Senior Aeronautical Engineer, Lockheed Martin Aeronautics Company, 1011 Lockheed Way, Palmdale, CA 93550; uribarri@princeton.edu.

†Chief Scientist, Electric Propulsion and Plasma Dynamics Laboratory; Professor, Mechanical and Aerospace Engineering Department; choueiri@princeton.edu. Associate Fellow AIAA.

results, and then present a model useful for generating voltage hash with the same statistics as those we see in our data. Throughout, we will make reference to anode spots (that is, small regions of enhanced current conduction at the anode) as a basis for explaining aspects of voltage hash and anode damage.

We begin in Sec. II by describing the specific MPDT system used in this paper. Section III describes the voltage hash in a statistical sense, using the probability distribution and power spectra of the signals at various $J^2/\dot{m}$. Also in Sec. III, we explain the origin of nonstationary statistics using high-speed video to capture the effect of anode vapor jets on the voltage hash. In Sec. IV, we present some observations of the anode damage caused by onset and describe how these are consistent with the observations of voltage hash. Section V describes a model that we use to generate signals that accurately represent voltage hash, with the whole range of observed statistics, and use that model to gain some insight into the behavior of anode spots with changing $J^2/\dot{m}$.

II. Benchmark MPDT

A. Full-Scale Benchmark MPDT

The full-scale benchmark MPDT (FSBT) system used in this study has been used since 1983 in extensive studies of thruster performance [1,21], electrode erosion [22], and plasma properties. The dimensions of the thruster are shown in Fig. 1. For the experiments in this paper, the thruster was fed with argon propellant at rates of 3 and 6 g/s, equally split between the cathode annulus and the outer ring of 12 holes shown in the figure (we will, however, use the well-known MPDT scaling parameter $J^2/\dot{m}$ to present all data, so that the mass flow rate will not appear explicitly). The cathode is 2% thoriated tungsten, the anode is made of various materials (as we shall discuss), and the insulating surfaces are Pyrex and boron nitride.

The FSBT is operated in quasi-steady fashion, in which steady-state operation is simulated by providing the thruster with a square current pulse long enough to allow plasma properties to become steady, but short enough that extensive thermal management infrastructure and a prohibitively high-current dc power supply are unnecessary. The current pulse is supplied by a pulse-forming network (PFN) with a 12.9 mF total capacitance and 14.9 μH total inductance. This PFN supplies 1 ms flat-topped pulses of current up to 25 kA. A stainless steel ballast resistor matches the impedance of the thruster to that of the bank, preventing the current from ringing during the pulse. An air-fed gas switch prevents the full PFN voltage from dropping across the thruster until triggered.

The voltage across the thruster is measured as physically close as possible to the thruster electrodes, to eliminate the influence of power-supply noise [23]. The signal is digitally sampled by a recording oscilloscope at a rate of 40 ns per point, for a Nyquist frequency of 12.5 MHz. Before digitization, the signal is filtered by a six-pole low-pass filter with a cutoff frequency of 5 MHz.

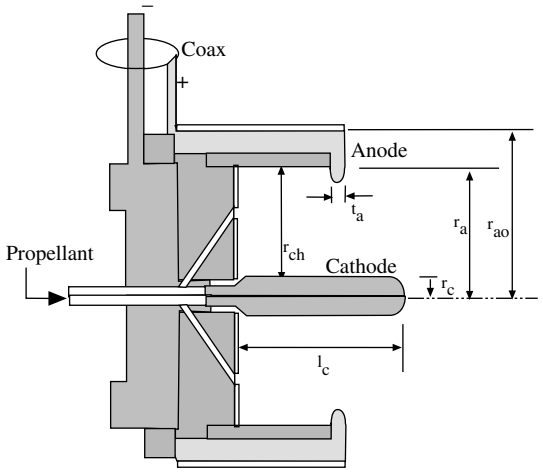

Fig. 1 Benchmark MPDT; $r_c = 0.95$ cm, $r_a = 5.1$ cm, $r_{ao} = 9.3$ cm, $r_{ch} = 6.4$ cm, $t_a = 0.95$ cm, and $l_c = 10$ cm.

In Sec. III.C, we present frames of a high-speed video taken of the thruster during an above-onset firing. The videos from which the presented frames were selected were taken with a Photron Ultima APX high-speed video camera at 50,000 frames per second. The light entering the camera was bandpass-filtered at 630 nm to attenuate propellant (argon) emission and allow anode (copper) emission from the arc. The camera was triggered by an auxiliary output of the recording oscilloscope, so that the videos were synchronized with the voltage data acquired.

B. FSBT Anode Materials

The anodes used in the FSBT for this study were made of four materials: copper, aluminum, lead, and graphite. Copper and aluminum have been the most recently used to study the near-anode plasma parameters in the FSBT [19], but the thermal properties of these two materials are quite similar with respect to the full range available in metals. Lead, for example, melts at 601 K, whereas graphite does not melt at all.

Regarding the interaction of the anode with the discharge, the most relevant measure of the difference between materials is the erosion rate. The erosion rate into vacuum of any material is a function of the temperature (derivable from kinetic theory) and is given in SI units by

$$\Gamma = p_{\text{sat}} \sqrt{\frac{M}{2\pi k T}} \tag{1}$$

where p_{sat} is the equilibrium vapor pressure. Empirical curves are available for p_{sat} for all of the preceding four materials [24,25]; using these (with the three metals in the liquid phase, and graphite solid), we calculate the erosion rate Γ for each as plotted in Fig. 2.

It is clear that copper and aluminum have very similar erosion rates over the range of temperatures that the anode experiences in the FSBT, in comparison with the difference between lead and graphite. An FSBT operating with a lead anode will have significantly more interaction between the arc and the anode than one operating with a graphite anode. The wide disparity in erosion rates will highlight the influence of erosion on onset voltage hash, as we will discuss.

III. Properties of Onset Voltage Hash

The 1 ms current pulse described in the last section is provided by a PFN of sufficient inductance that the current does not change appreciably if the thruster impedance varies during the course of a firing. The hallmark of the onset problem is that although the thruster impedance is constant (about 10 mΩ) during a firing at low currents, the impedance changes rapidly at high currents, which, due to the stiff current source, causes the voltage to do the same. In the FSBT, this transition occurs at $J^2/\dot{m} \sim 60$ kA$^2 \cdot$ s/g. The magnitude of this fluctuation grows rapidly, beginning at a higher value of

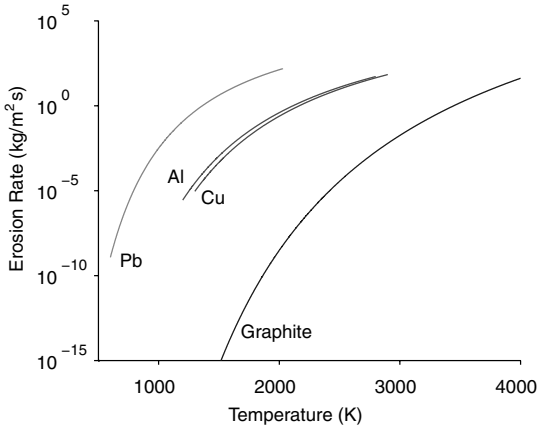

Fig. 2 Erosion rate of four anode materials as a function of temperature.

$J^2/\dot{m} \sim 80$–100 kA$^2 \cdot$ s/g. Examples of the voltage hash after each of these transitions are shown in Fig. 3.

As discussed in the last section, we have obtained voltage hash using anodes of several materials. In what follows, we will discuss the hash obtained with copper, lead, and graphite anodes.

A. Statistics of Voltage Hash

The voltage hash that we have measured in this study is a random fluctuation. Random is a technical descriptor that indicates that no deterministic (that is, transient or periodic) function can be used to describe the fluctuation of the voltage during periods of hash. The distinction between periodic and random data can be made based upon whether peaks appear in the power spectrum: as we will see, this is not the case for our voltage hash. At the same time, it is clear that our voltage hash is not a transient function of time.

The analysis of random signals is more complex than the corresponding analysis of deterministic signals [26]. Whereas a deterministic signal is described by an equation with parameters that can be determined by analysis of the signal (and presumably varied by alterations to the experiment), random data must be analyzed in a statistical sense. Statistics generally calculated in the process are the mean, the spectral density, and the probability density of the signal (which is often Gaussian about the mean, but can differ significantly from this baseline).

We will use this analysis to describe our voltage hash. However, applying these measures to the analysis of voltage hash presents unique challenges because each signal is nonstationary, and the statistics are therefore not constant over the duration of each signal. For example, perhaps the most obvious feature of the voltage traces of Fig. 3 is that the voltage hash is not of constant amplitude over the course of the firing. This is not the normal behavior of hash amplitude during a firing; in fact, there is no normal behavior that we can ascribe to the time variation of the hash amplitude. In a series of firings under identical experimental conditions, the hash may last for the entire quasi-steady portion of the firing or may begin and end one or more times in bursts throughout the firing. As we will discuss, this behavior has to do with the release of vaporized anode material into the discharge. We cannot, however, control this behavior by any standard modifications to the MPDT: its circuit elements, anode condition, or propellant. As a result of this variability, the statistics that we calculate for the voltage hash exhibit a degree of scatter.

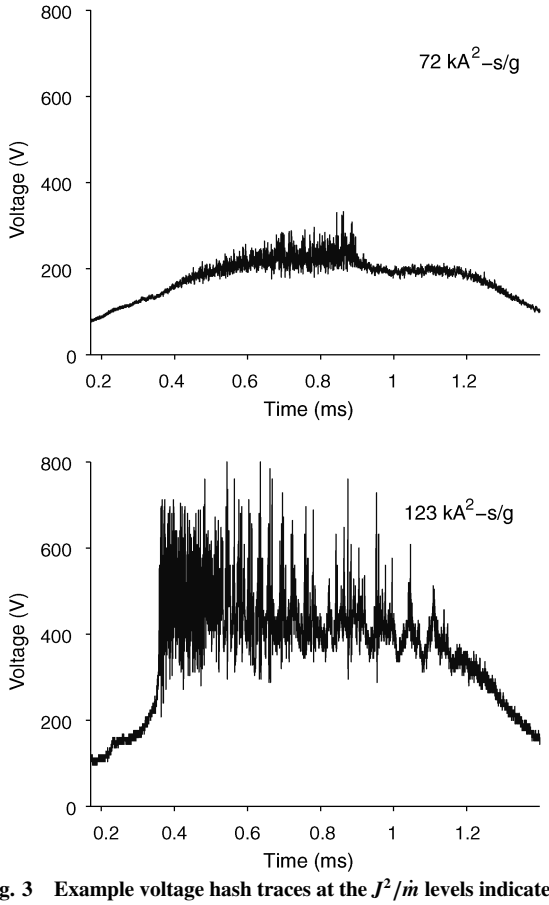

Fig. 3 Example voltage hash traces at the $J^2/\dot{m}$ levels indicated.

Our analysis proceeds as follows. For each voltage hash trace as in Fig. 3, we take a portion of the trace corresponding to the time of the quasi-steady current (which lies between 0.4 and 1.2 ms) and calculate the probability distribution of the signal during a 0.3 ms portion of this time, from 0.8 to 1.1 ms (doing so is important to avoid startup and shutdown transients, which can be longer in the voltage signal than they are in the current and can cause significant scatter in the statistics). For better spectral resolution, we calculate the power spectra using the entire quasi-steady period. The statistics and spectrum of each signal are then averaged over several firings: six for the copper anode and nine for the graphite. Error bars on all such quantities represent the scatter in the data. The exception to this rule are data taken with a lead anode, which sustains significant damage on each firing. Only a single firing was taken with lead at each $J^2/\dot{m}$, so that these data lack error bars and the power spectra have greater spectral noise.

B. Results

The mean, standard deviation, skewness, and kurtosis (the first four standardized moments) of the voltage hash obtained with copper, lead, and graphite anodes are shown as functions of $J^2/\dot{m}$ in Fig. 4. The signal mean is the average voltage over the course of a firing. The standard deviation is a quantitative measure of the amplitude of the hash: for a Gaussian distribution, 95% of the voltage signal would be contained within 2 standard deviations of the mean. Using this measure rather than a peak amplitude guards against overestimating the hash magnitude in cases in which an outlying fluctuation is much larger than the typical fluctuations.

The skewness is the measure of any long tails on either the positive or negative side of the distribution average. A positive skewness indicates that a signal spends more time above the mean value than a Gaussian signal would. (A Gaussian distribution, which has no long tails, has a skewness of zero.) The kurtosis of the signal is the measure of how peaked or biased the signal is toward small values. A signal that spends much time near the mean with short-duration large excursions away will have a positive kurtosis. (Again, a Gaussian distribution has a kurtosis of zero, in our definition; other definitions assign a Gaussian a kurtosis of 3.)

The plot of the mean values is a classic voltage-current characteristic of the self-field FSBT [1]. We will not dwell on this, except to mention that at the highest currents, a lead anode appears to operate at a lower voltage than the others. Because lead provides a more copious supply of evaporated material to the discharge than the other anodes, the plasma density near a lead anode will likely be larger than that near an anode of another material, and lower voltages would be necessary to drive equivalent current through this more-conductive plasma. This may be seen as equivalent to having a higher effective $\dot{m}$.

The standard deviation of the voltage signals follows the same trend over the range of current for all three anodes. It is somewhat surprising that the magnitude of the hash, or the $J^2/\dot{m}$ level at which it grows significantly, is apparently insensitive to very different anode materials. Anode evaporation, after all, has been associated with voltage hash many times in the past, and it is reasonable to think that the one affects the other. On the other hand, it is also possible that the voltage hash arises independently of the anode damage, which is itself a passive thermal response of the anode to the mechanism behind the hash. We will explore one such possible mechanism in Sec. V.

The skewness and kurtosis of the hash also follow similar trends among the materials. Each hovers around zero over most of the current range, before rising to large positive values at the $J^2/\dot{m}$ at which the standard deviation begins rising significantly. This

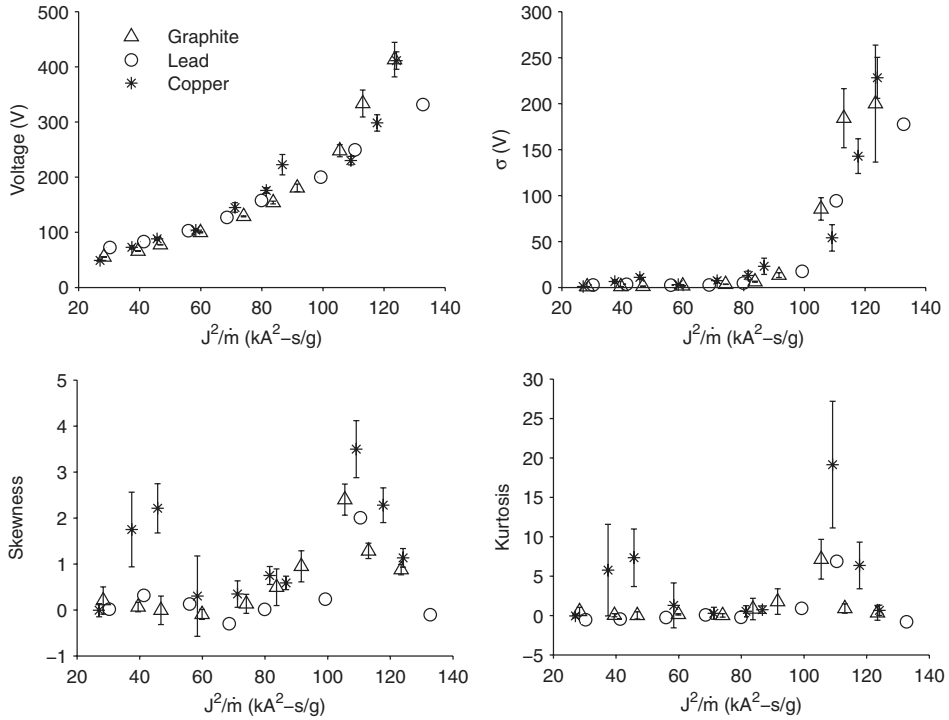

Fig. 4 Voltage statistics for three anode materials.

happens because, as the hash grows between the magnitude levels in the two panels of Fig. 3, the fluctuations first resemble infrequent large positive excursions away from the mean. As $J^2/\dot{m}$ rises further, these excursions become more frequent and begin to overlap, bringing the skewness and kurtosis statistics back toward their Gaussian levels. That the excursions occur above the mean gives rise to the positive skewness; the positive kurtosis occurs because the excursions rise and fall quickly. This behavior indicates that the random fluctuations in the voltage arise from ascending spikes, which relax quickly to small values. Again, we will discuss one possible origin for this behavior in Sec. V.

The skewness and kurtosis for copper have a brief excursion away from zero at low $J^2/\dot{m}$ values. This is because hash with a copper anode, unlike that with lead and graphite, does not arise smoothly out of low-current quiescent operation, but first occurs in short bursts during a single firing. This is likely due to the influence of anode erosion, which we will see in Sec. III.C. Refractory graphite may not erode enough to affect the hash in the same way, whereas lead may erode more continuously, so that the effect on the hash does not change during the firing. Copper, which erodes in bursts, as we will see, lies in the middle of those two extremes.

The similarity of the statistics for the three anodes is paralleled in the similarity of the power spectra for the same three anodes, an example of which we give in Fig. 5. All three spectra display the same $1/f^{\beta}$ characteristic fall, with $1 < \beta < 2$; superimposed on each plot in Fig. 5 is a line representing $f^{-3/2}$ to highlight the similarity. (Periodic content at 1.3 MHz is noise associated with the power supply [23].) The frequency range over which the $1/f^{\beta}$ persists, from about 10–100 kHz to 1 MHz, covers the timescales associated with the peaks and valleys identifiable as voltage hash. Lower frequencies than these correspond to long-time trends in the voltage traces, such as are caused, for example, by the anode evaporation discussed in the next section. (Note that, for the reasons discussed in the preceding section, the lead spectrum was calculated using a single voltage trace and contains a significant amount of spectral noise. This noise can serve to obscure the $1/f^{\beta}$ trend, more clearly in evidence in the copper and graphite spectra, which are both averages over several shots.)

The $1/f^{\beta}$ characteristic fall in the spectra is characteristic of a Brownian motion ($\beta = 2$ is true Brownian motion, and $\beta < 2$ is a fractional Brownian motion) and is revealing with regard to the mechanism behind the hash [27]. Whereas a white noise process, which has a flat spectrum, is generated by choosing a random value for each point in the signal, a Brownian motion (specifically, for $\beta = 2$) is generated by choosing a random value for the *slope* between each two points in the signal, and hence the Brownian motion is the integration of white noise. The spectrum of an integrated white noise signal falls off with a slope $\beta = 2$. As we consider the physical process behind the voltage hash, therefore, we must keep in mind that the underlying randomness in the signal is not in the sampled voltage values themselves, but in the voltage change between consecutive samples. We will use this insight in Sec. V to develop a random model for the hash.

C. Origin of Nonstationary Statistics

We have already noted that the statistics of the voltage hash are nonstationary: that is, they change over the course of a single quasi-steady firing. In this section, we show that the nonstationarity is a result of anode evaporation, which, if severe enough, can suppress the hash. To demonstrate this, we captured high-speed video of the copper light emission from the thruster plume, synchronized with acquisition of the thruster voltage.

A representative example of our video footage appears in Fig. 6. This shows (top) a portion of a voltage trace for a thruster firing with a copper anode at $J^2/\dot{m} = 60\ \mathrm{kA}^2 \cdot \mathrm{s/g}$, labeled on the abscissa with numbers corresponding to the numbered frames of the high-speed video shown (bottom) in the figure. These frames, each of which captures 20 μs, have been inverted and contrast-enhanced, so that dark regions correspond to copper emission and white regions correspond to darkness. To orient the reader, a dotted circle in the first frame represents the internal edge of the anode, and the cathode is the white area surrounded by black pixels. The intervening area is the discharge chamber. As suggested by Rudolph [3], it is likely that the luminosity surrounding the cathode in each frame is not the result of line emission by copper vapor, but rather of continuum radiation originating in the hot high-density plasma near the cathode and within the barrel structure that stands roughly 1 cm off the cathode.

The pattern revealed in our videos is clear: the emission of anode vapor in jets that arrive at the cathode tends to suppress the voltage hash, which drops to a small fraction of its magnitude whenever the

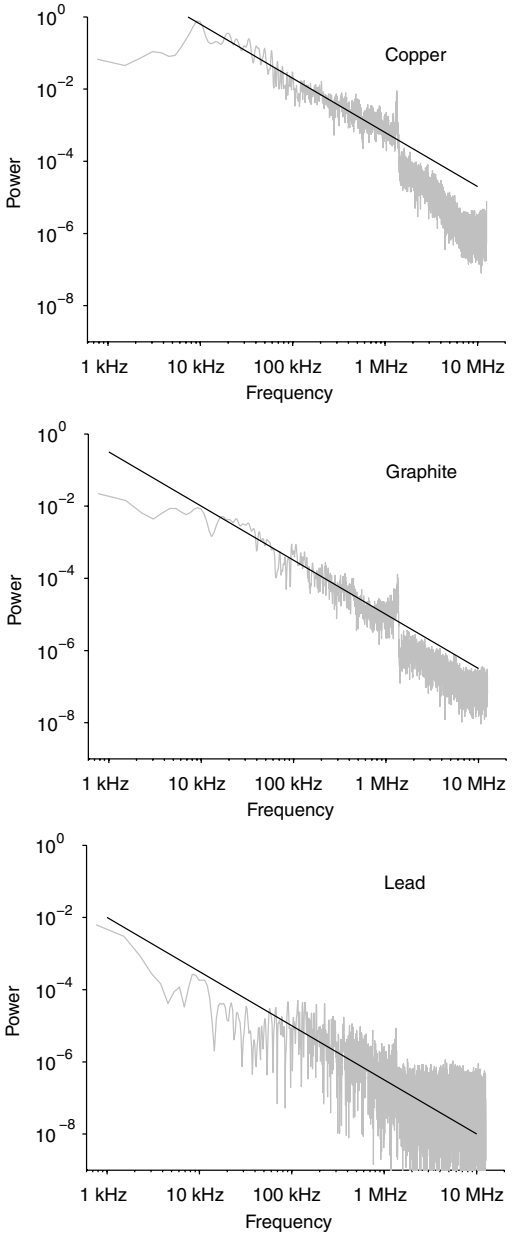

Fig. 5 Example power spectra for all three anode materials, for operation at $J^2/\dot{m} = 66\ \mathrm{kA^2 \cdot s/g}$. Superimposed on each plot is a line representing $f^{-3/2}$.

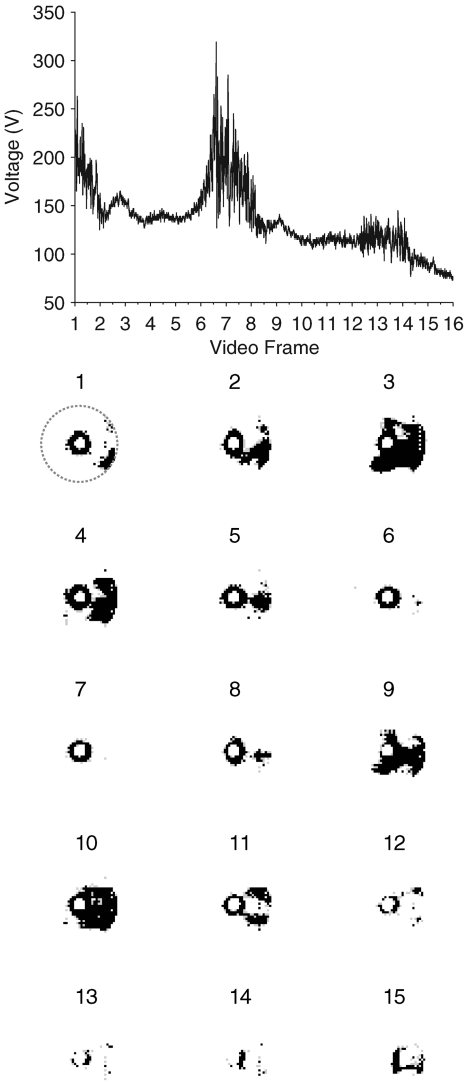

Fig. 6 The 0.3 ms portion of a voltage trace at $J^2/\dot{m} = 60\ \mathrm{kA^2 \cdot s/g}$ and the corresponding frames of a high-speed video capturing copper light emission.

eroded copper forms a bridge between the anode and cathode, as in frames 9 and 10. On the other hand, the periods in which large-amplitude voltage hash exists correspond to the periods in which eroded anode material does not form such a bridge. This is consistent with the observation from vacuum interrupter literature that voltage hash in vacuum arcs is suppressed when the evaporated material in an anode jet bridges the gap between anode and cathode [28].

IV. Properties of Onset Anode Damage

We have so far discussed the voltage hash, noting that it is a random fluctuation with statistics that evolve with $J^2/\dot{m}$ but that are not greatly altered by the choice of anode material. This finding argues that the voltage hash exists, to a great extent, independently of the damage to the anode and that the anode is therefore a passive responder to the mechanism behind the hash (this, with the exception that sufficient erosion can suppress the hash, as we saw in the last section).

Anode damage manifests itself as individual spots or streaks distributed all over the anode surface, but preferentially at anode-insulator boundaries and along the anode inner lip. The distribution of damage marks over the surface is not azimuthally symmetric. The severity of the damage is a strong function of the anode material: the more refractory the material, the less damage appears. Graphite, for example, shows no evidence of significant damage for all operating conditions, even the highest $J^2/\dot{m}$; lead, on the other hand, shows significant melting for even the lowest $J^2/\dot{m}$. Aluminum and copper fall in between.

Though the damage that appears on the several anode materials we have used is of the same quality (spots and streaks, melting, and discoloration), aluminum is the best material of the four on which to make careful observations of the damage, for it visibly melts more than copper, but not as easily as lead. The damage appears in a variety of sizes on the anode surface, and we are interested in the distribution of the sizes: how many marks of each size appear. To measure the distribution of damage point sizes, we subjected a polished aluminum anode to two above-onset firings. We then, under optical magnification, recorded the number and sizes of damage marks over the entire anode surface. The photographs in Fig. 7 show examples of the damage points included in the counting. We define the size of a mark to be the diameter for roughly circular marks, or the long dimension for oblong marks. After categorizing the damage points by size, these were binned according to the sizes of the points, one bin per order of magnitude. The result is the four-point histogram shown in Fig. 7.

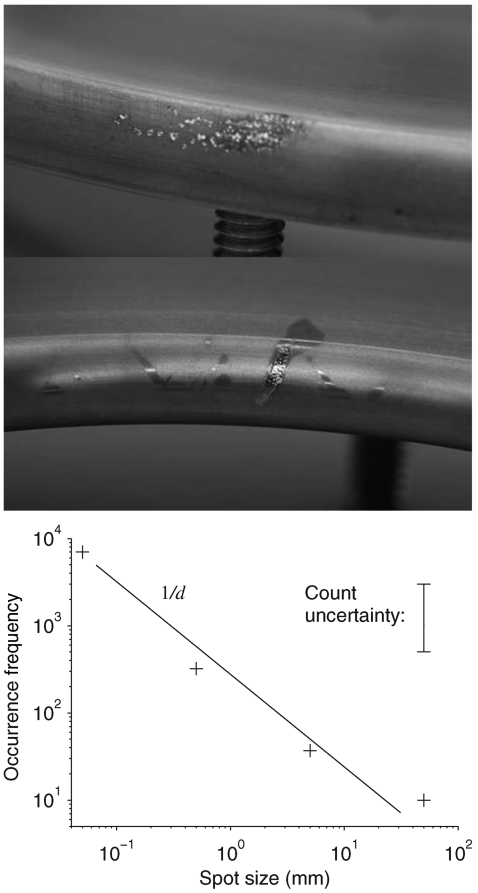

Fig. 7 Damage along outer edge (top) and inner lip (middle) of the aluminum anode and distribution of damage mark sizes from two above-onset firings on the aluminum anode (bottom).

Within the range of damage sizes that we have cataloged, there is no preferred size. Instead, there is a distribution of sizes following the power law $1/d$, where d is the spot size. The line $1/d$ is plotted along with the data points in the log–log plot of Fig. 7.

The range of spot sizes examined is limited on the large end by the largest mark size observed, which is likely related to the length of the current pulse. The limit on the low end is due to the difficulty in positively identifying damage left behind by the arc: at sizes smaller than those in the figure, marks left behind by the polishing process and, more significantly, those caused by oxidation and corrosion of the surface can appear to be very similar to arc damage. Investigation of smaller sizes requires a higher degree of anode surface polish than was possible in these experiments on an anode made of a suitable metal (one that is noncorrosive in air and has appropriate thermal properties).

The negative slope of the points in Fig. 7 is artificially low, because large marks inevitably obliterate small marks. For this reason, the count in the range 1–10 mm is lower than it would be had not some of those marks been obliterated by those in the 10–100 mm range; the count is, for the same reason, too low in the 0.1–1 mm range, and so forth. Although the distribution therefore has a slope close to -1 on the logarithmic scale shown in the figure, it is likely that the distribution of mark sizes decreases as $1/d^{\delta}$, where $\delta \geq 1$.

That there is no characteristic damage size indicates that there is no characteristic energy delivered to the anode by a single spot: that is, no characteristic power in the spot and no characteristic spot lifetime. This is consistent with our observation that there is no characteristic timescale in the voltage hash, but rather a power-law drop in hash signal power with increasing frequency (decreasing timescale). As we might expect that a characteristic hash timescale would lead to a characteristic damage mark size, the lack of characteristic values in both of these observations is satisfying.

V. Origin of Voltage Hash

A. Model of Random Superposition of Events

Because the voltage hash, as we have presented it in the preceding sections, is an essentially random process, modeling based on deterministic mathematics is inappropriate. Instead, in this section, we will offer an explanation for what is occurring during voltage hash based upon a random superposition of events that are likely to occur in a current-starved MPDT that is susceptible to anode spotting.

Anode spots differ from the better-understood cathode spots in that they are not the sole conductors of current to the anode, whereas arc current from a cold cathode is usually collected solely in a number of spots. Current to the anode may also be diffusely collected. In this sense, the definition of an anode spot is a local region on the anode surface of higher current density (higher conductivity) than the surrounding, diffuse regions.

Because an anode can only collect an amount of current up to the electron saturation current diffusely, any further current driven through the anode will either be conducted by spots or will appear as a voltage rise across the anode sheath. The sheath/spot interaction can be thought of as the parallel combination of the sheath capacitance and the spot resistance. Figure 8 shows this parallel combination and a switch for which the opening and closing represent the extinction and ignition of a spot, respectively. The indicated current I_e is the difference between the electron saturation current of the MPDT anode/plasma combination (diffuse current collection) and the current being driven through the thruster by the PFN ($I_e = I_{\mathrm{PFN}} - I_{\mathrm{sat}}$).

If the power supply is sufficiently inductive (stiff), as in our experiment, then I_e is unaffected by the change in voltage across this combination as the capacitor charges and discharges. The voltage across the capacitor when the switch is opened therefore rises linearly with time and is

$$V_c = \frac{I_e}{C_s} t \tag{2}$$

When the switch closes, the voltage across the combination falls as the capacitor discharges through the resistor, according to

$$V = V_c e^{-t/R_s C_s} \tag{3}$$

The ratio of the rise and fall times of the voltage is $V_c/R_s I_e$. Experimental measures of I_e are impossible to obtain, but because we do not, in general, observe voltage rise rates of greater than 100 V/μs, and the value of the sheath capacitance is on the order of 100 nF [29], I_e is likely no larger than ~10–100 A. Because the resistance of the thruster plasma as a whole is on the order of 10 mΩ, and R_s should be smaller than this value, we expect that in a typical spotting cycle, the rise time will be longer than the fall time. Experimentally as well, we observe voltage fall times to be much shorter than the rise times when we are able to distinguish individual rises and falls.

A single spotting event will therefore look something like the ramp in Fig. 9a, in which the specific values of time and voltage are

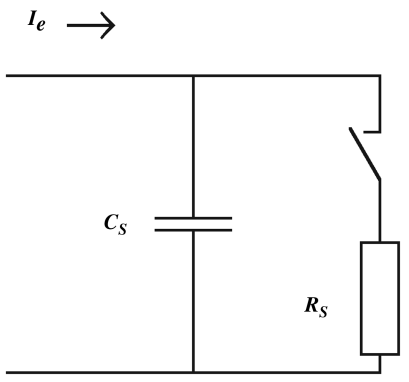

Fig. 8 Parallel *RC* model of anode sheath and single spot.

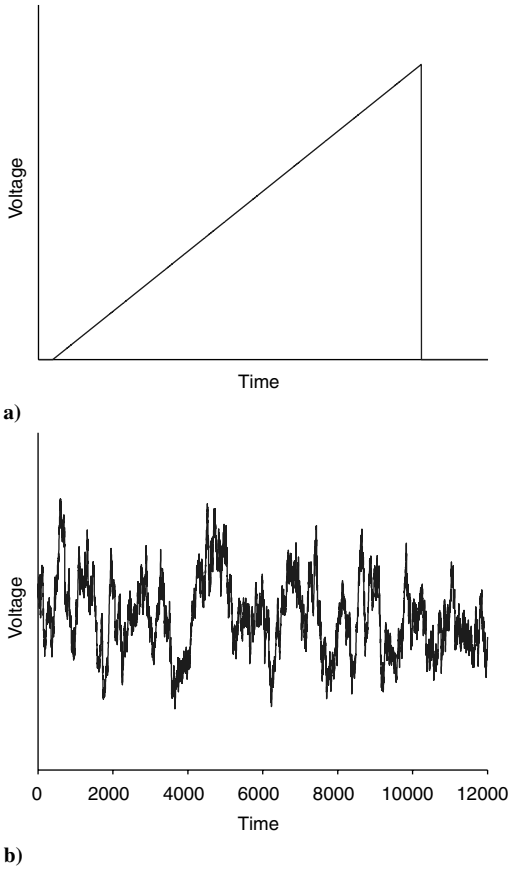

Fig. 9 Voltage change caused by a) a single starvation/spotting event and b) random superposition of many such events. In this figure, all units are arbitrary.

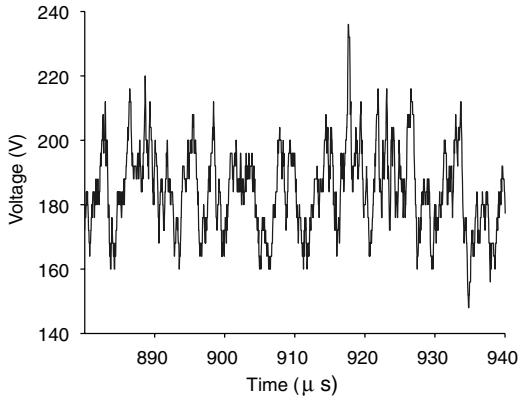

Fig. 10 Experimental realization of voltage hash, for comparison with the simulated signal in Fig. 9b. $J^2/\dot{m} = 72\ \mathrm{kA^2 \cdot s/g}$.

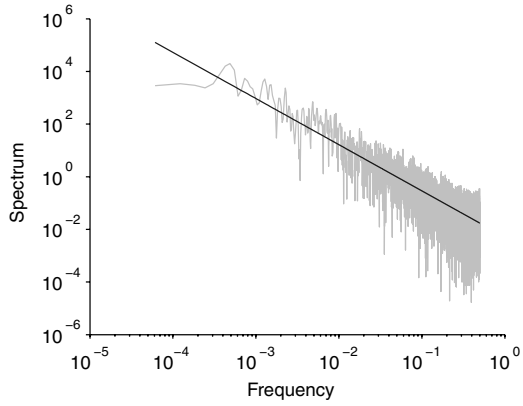

Fig. 11 Power spectrum of the signal in Fig. 9b.

dependent upon the parameters and the fall time here is shown much smaller than the rise time.

If we take this process to be indicative of what occurs across the anode sheath in the MPDT, then a full picture will include many anode spots (and the number may change with time), each having their own resistance R_s, but all sharing the same sheath capacitance C_s. The voltage that we measure across C_s will therefore be the superposition of the activity of all the spots or, in the parlance of our model, the superposition of many switching events.

The picture we propose is consistent with our experiment under the following conditions:

1) The current carried by each spot is sheath-limited in its steady state. This ensures that when a spot extinguishes, the current it had carried goes to charging the sheath capacitance, rather than being redistributed to other spots. Were this not the case, we would expect no more than one high-conductivity spot to form, inconsistent with our observations.

2) The spotting events are uncorrelated. It is not immediately apparent, in a physical context, in what way distant spots would communicate strongly with one another, and so we expect this assumption to be reasonable.

If we now take a random superposition of many events such as that in Fig. 9a, the signal that we generate appears as that in Fig. 9b. This particular instance is a segment of a signal generated by 4096 events randomly distributed into a time span of 16,384 (in which the units are arbitrary). The rise times were randomly distributed between 2 and 512, and the amplitudes were chosen randomly on the interval [0, 1]. The vertical axis remains unlabeled, as the amplitude of the signal can be arbitrarily scaled with the maximum event amplitude chosen. As a comparison, a segment of a real voltage trace exhibiting hash, for $J^2/\dot{m} = 72\ \mathrm{kA^2 \cdot s/g}$, is shown in Fig. 10.

The generated signal in Fig. 9b is a realistic reproduction of the voltage hash. This signal is, like the voltage hash, a random walk, generated by the random superposition of deterministic functions. The power spectrum of this signal is shown in Fig. 11. The superimposed fit line on this graph corresponds to the function $1/f^{1.75}$: the power spectrum of the generated noise has a power-law drop for which the exponent is, like those of the experimental voltage hash, between 1 and 2. Clearly, by randomly superimposing many linear rises in this way, we have created a signal for which the slope between any two points is a random variable. As we discussed in Sec. III.A, this gives rise to a Brownian motion such as the one we have just calculated.

The statistics of our generated signal depend upon the average occurrence rate n of the events and upon the rise time τ of the events. The mean and standard deviation, as we have already pointed out, can be arbitrarily scaled according to the characteristic amplitude of the events; the skewness and kurtosis of the signals, on the other hand, show a tendency toward zero as the product $n\tau$ rises; that is, the signal becomes more Gaussian as the events increasingly overlap. These trends are shown in Fig. 12. The range spanned by these statistics cover the entire range of statistics calculated for the experimental voltage hash in Sec. III.A.

B. Discussion

We can use our understanding of this simple model to gain some physical insight from the experimental hash statistics. Both the skewness and kurtosis of the experimentally measured hash evolve with $J^2/\dot{m}$, both reaching a peak at the same $J^2/\dot{m}$ value. We can picture the evolution of the statistics from Gaussian to a distribution with significant skewness and kurtosis and then back toward a Gaussian as a movement first to the left, then back to the right, along the curves of Fig. 12. This indicates that the product $n\tau$ first decreases as $J^2/\dot{m}$ increases and then reverses. Physically, we may understand this in the following way. The occurrence frequency n is related to the average number of spots that are carrying current during a thruster firing: it is the ignition, and extinction, of these spots that create a

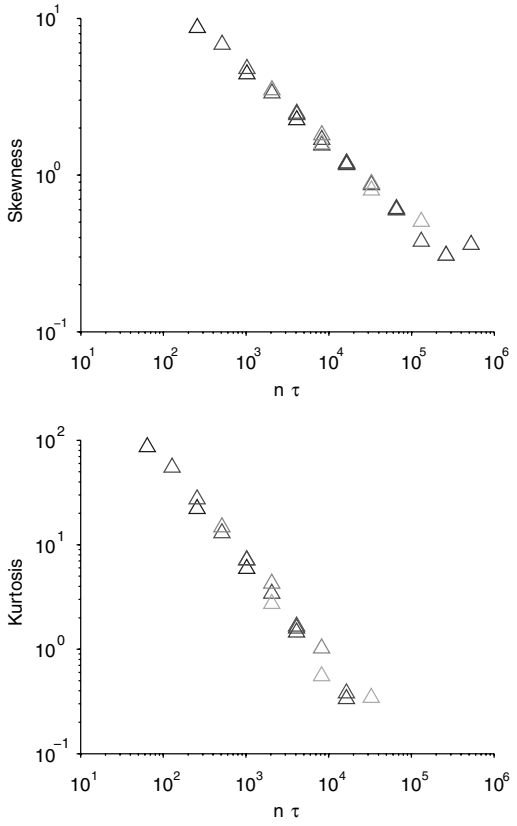

Fig. 12 Skewness (top) and kurtosis (bottom) of generated signals with various $n\tau$ values.

single event. The rise time τ is representative of the current carried by a spot; the higher the current, the greater the slope of the voltage rise when the spot extinguishes, and the shorter the rise time if the voltage is not to increase to arbitrarily large values. Our data suggest that at first τ falls faster with current than n rises, so that $n\tau$ falls, and the hash statistics become significantly skewed from Gaussian. At sufficiently high current, however, increasing n catches up with the falling τ, so that $n\tau$ falls again and the statistics return toward Gaussian.

The implication of this for our understanding of anode spotting and voltage hash can be simply stated. To carry increasing thruster current in the anode-starved onset condition, anode spots must either carry more current each or a greater number of anode spots must form. Our evidence suggests that in the intermediate $J^2/\dot{m}$ range, the current carried (or spot size) first grows in response to increasing thruster current; past a particular $J^2/\dot{m}$ ($\sim$110 kA$^2 \cdot$ s/g, in our data), the number of spots then increases. Although it is likely that this is a general trend among MPDTs, the specific value of $J^2/\dot{m} \sim$ 110 kA$^2 \cdot$ s/g is specific to the FSBT geometry and argon propellant and will change as the geometry or propellant of the MPDT is altered.

This interpretation of Fig. 4, in which we associate the return of the statistics toward Gaussian with an increasing number of anode spots, implies that in the FSBT an effective mechanism for anode spot creation becomes dominant at $J^2/\dot{m} \sim 110$ kA$^2 \cdot$ s/g. Because this $J^2/\dot{m}$ value is independent of the anode material, we expect that this mechanism is a plasma phenomenon. It is possible that anode spots, as described here and in the references, are a manifestation of current filamentation, which is observed in coaxial plasma accelerators such as the plasma focus [30,31]. Such current filaments exhibit some of the properties that we have inferred about anode spots, such as a limit on the filament current [31]. A number of mechanisms, such as thermal instabilities and ion-acoustic instabilities, can give rise to filamentation in plasmas [32,33]. As $J^2/\dot{m}$ rises (and with it, the electron drift velocity and the specific power input to the plasma), one of these instabilities may be excited, and the current will filament, increasing the number of unsteady anode spots. Should a detailed study of the relevant threshold parameters for these instabilities uncover one such threshold that is equivalent to $J^2/\dot{m} \sim$ 110 kA$^2 \cdot$ s/g in the FSBT, this will support our hypothesis that the mechanism behind the increasing number of anode spots after this $J^2/\dot{m}$ value is current filamentation.

VI. Conclusions

It was our intention in this paper to describe the nature of voltage hash in a quantitative manner, to describe the relationship of the voltage hash to the anode damage further than we have earlier [20], and to describe a model of the voltage hash that can explain our observations and provide some insight into the MPDT onset physics that we cannot easily observe.

The voltage hash is a random signal, demonstrated by its power spectrum that lacks evidence of periodicity and the evidently nontransient nature of the signal. The statistics and power spectra of the hash for three anode materials with widely different material properties were not significantly different from one another. The FSBT voltage hash statistics evolve with $J^2/\dot{m}$, moving first away from Gaussian until $J^2/\dot{m} \sim 110$ kA$^2 \cdot$ s/g, and falling back toward Gaussian afterward. The power spectra have a characteristic $1/f^{\beta}$ fall in power, as is representative of a Brownian-type motion. Nonstationarity of the statistics is due in large part to the influence of jets of anode material bridging the gap between anode and cathode.

We have presented a model, based upon the superposition of random anode spot events, that shows the same Brownian-type motion as the experimental data, and that, depending upon the model parameters chosen, can exhibit the same statistics as the data. By associating our model parameters with the properties of anode spots (that is, the total number of spots and the current carried by the spots in a single firing), we infer from the evolution of our hash statistics that as the current through the thruster increases, the current carried by each of a small number of spots first increases, and only after that has taken place does the number of spots increase.

Finally, it is important to point out that our task in this paper has been to use the a priori knowledge that anode spots *do* form and *are* unsteady to deduce what the effect of the unsteady anode spots will be on the discharge voltage. Important questions we have left open relate to *why*: Why do anode spots form, and why are they unsteady once they do? These questions are the appropriate subject of a fundamental study of anode spotting, one that perhaps uses an experimental setup different from the FSBT, the geometry of which makes it difficult to reliably capture precise local information on the randomly forming anode spots. We are not familiar with any such study bearing conclusive answers to these questions that was carried out in an operating regime similar to that of the FSBT.

The insights in this paper may be applicable to attempts to control voltage hash. If, as our findings suggest, the statistics of the hash are governed by the number of anode spots and the current carried by each spot, then deliberately influencing either of these quantities should allow for control of the hash statistics. For example, an anode insulated everywhere but in a discrete number of points (so forcing the anode attachment to be in a certain number of spots) may exhibit a constrained range of hash statistics. If such a constraining of the anode attachment were to stabilize the spots, so that they did not extinguish often, this could also have the effect of suppressing the voltage hash.

Acknowledgments

The authors would like to thank the National Defense Science and Engineering Graduate Fellowship program, the Princeton Program in Plasma Science and Technology, and the Wallace Memorial Fellowship fund for support at various points during this work. We would also like to acknowledge the invaluable technical assistance of Bob Sorenson.

References

[1] Choueiri, E. Y., and Ziemer, J. K., "Quasi-Steady Magneto-plasmadynamic Thruster Performance Database," *Journal of Propulsion and Power*, Vol. 17, No. 4, Sept.–Oct. 2001, pp. 520–529.

[2] Malliaris, A. C., John, R. R., Garrison, R. L., and Libby, D. R., "Performance of Quasi-Steady MPD Thrusters at High Powers," *AIAA Journal*, Vol. 10, No. 2, Feb. 1972, pp. 121–122. doi:10.2514/3.50074

[3] Rudolph, L. K., "The MPD Thruster Onset Current Performance Limitation," Ph.D. Thesis, Princeton Univ., 1980.

[4] Boyle, M. J., Clark, K. E., and Jahn, R. G., "Flowfield Characteristics and Performance Limitations of Quasi-Steady Magnetoplasmadynamic Accelerators," *AIAA Journal*, Vol. 14, No. 7, July 1976, pp. 955–962. doi:10.2514/3.61435

[5] Shubin, A. P., "Dynamic Nature of Critical Regimes in Steady-State High-Current Plasma Accelerators," *Soviet Journal of Plasma Physics*, Vol. 2, No. 1, Jan.–Feb. 1976, pp. 18–21.

[6] Wagner, H. P., Kaeppeler, H. J., and Auweter-Kurtz, M., "Instabilities in MPD Thruster Flows, 1: Space Charge Instabilities in Unbounded And Inhomogeneous Plasmas," *Journal of Physics D: Applied Physics*, Vol. 31, 1998, pp. 5–19.

[7] Zuin, M., Cavazzana, R., Martines, E., Serianni, G., Antoni, V., Bagatin, M., Andrenucci, M., Paganucci, F., and Rossetti, P., "Critical Regimes and Magnetohydrodynamic Instabilities in a Magneto-Plasma-Dynamic Thruster," *Physics of Plasmas*, Vol. 11, No. 10, Oct. 2004, pp. 47–61.

[8] Hugel, H., "Flow Rate Limitations in the Self-Field Accelerator," 10th Electric Propulsion Conference, AIAA Paper 73-1094, 1973.

[9] Baksht, F. G., Moizhes, Y. B., and Rybakov, A. B., "Critical Regime of a Plasma Accelerator," *Soviet Physics Technical Physics*, Vol. 18, No. 12, June 1974, p. 1613.

[10] Diamant, K. D., "The Anode Fall in a High Power Pulsed MPD Thruster," Ph.D. Thesis, Princeton Univ., 1996.

[11] Korsun, A. G., "Current Limiting by Self Magnetic Field in a Plasma Accelerator," *Soviet Physics Technical Physics*, Vol. 19, No. 1, July 1974, pp. 124–126.

[12] Vainberg, L. I., Lyubimov, G. A., and Smolin, G. G., "High-Current Discharge Effects and Anode Damage in an End-Fire Plasma Accelerator," *Soviet Physics Technical Physics*, Vol. 23, No. 4, Apr. 1978, pp. 439–443.

[13] Hugel, H., "Flow Rate Limitations in the Self-Field Accelerator," *AIAA Journal*, Vol. 12, No. 11, November 1974, pp. 1461–1462. doi:10.2514/3.49527

[14] Kurtz, H. L., Auweter-Kurtz, M., Merke, W. D., and Schrade, H. O., "Experimental MPD Thruster Investigations," 19th International Electric Propulsion Conference, AIAA Paper 87-1019, 1987.

[15] Rudolph, L. K., Jahn, R. G., Clark, K. E., and von Jaskowsky, W. F., "Onset Phenomena in Self-Field MPD Arcjets," 13th International Electric Propulsion Conference, AIAA Paper 78-653, 1978.

[16] Ho, D. D., "Erosion Studies in an MPD Thruster," M.S. Thesis, Princeton Univ., 1981.

[17] Kuriki, K., and Iida, H., "Spectrum Analysis of Instabilities in MPD Arcjet," International Electric Propulsion Conference, AIAA Paper 84-28, 1984.

[18] Barnett, J. W., and Jahn, R. G., "Onset Phenomena in MPD Thrusters," 18th AIAA International Electric Propulsion Conference, AIAA Paper 85-2038, 1985.

[19] Diamant, K. D., Choueiri, Edgar Y., and Jahn, Robert G., "Spot Mode Transition and the Anode Fall of Pulsed Magnetoplasmadynamic Thrusters," *Journal of Propulsion and Power*, Vol. 14, No. 6, Nov.–Dec. 1998, pp. 1036–1042. doi:10.2514/2.5371

[20] Uribarri Luke, and Choueiri, Edgar Y., "Relationship Between Anode Spots and Onset Voltage Hash in Magnetoplasmadynamic Thrusters," *Journal of Propulsion and Power*, Vol. 24, No. 3, 2008, pp. 5–71. doi:10.2514/1.34525

[21] Burton, R. L., Clark, K. E., and Jahn, R. G., "Measured Performance of a Multi-Megawatt MPD Thruster," *Journal of Spacecraft and Rockets*, Vol. 20, No. 3, 1983, pp. 299–304. doi:10.2514/3.25596

[22] Polk, J. E., "Measurement of MPD Thruster Erosion Using Surface Layer Activation," *Journal of Propulsion and Power*, Vol. 3, No. 1, Jan. 1987, pp. 33–38. doi:10.2514/3.22949

[23] Uribarri Luke, and Choueiri, Edgar Y., "Corruption of Pulsed Electric Thruster Voltage Fluctuation Measurements by Transmission Line Resonances," *Journal of Propulsion and Power*, Vol. 24, No. 3, 2008, pp. 6–37. doi:10.2514/1.33865

[24] *The Industrial Graphite Engineering Handbook*, Union Carbide Corp., New York, 1969.

[25] Gale, W. F., and Totemeier, T. C. (eds.), *Smithell's Metals Reference Book*, 8th ed., Elsevier, New York, 2004.

[26] Bendat, Julius S., and Piersol, Allan G., *Random Data: Analysis and Measurement Procedures*, Wiley, New York, 2000.

[27] Schuster, H. G., and Just, W., *Deterministic Chaos*, Wiley-VCH, Berlin, 2006.

[28] Harris, L. P., "Small-Scale Anode Activity in Vacuum Arcs," *IEEE Transactions on Plasma Science*, Vol. 10, No. 3, Sept. 1982, pp. 173–180. doi:10.1109/TPS.1982.4316164

[29] Uribarri Luke, and Choueiri, E. Y., "The Onset of Voltage Hash and its Relationship to Anode Spots in Magnetoplasmadynamic Thrusters," 29th International Electric Propulsion Conference, AIAA Paper 2005-084, 2005.

[30] Milanese, M. M., Niedbalski, J. J., and Moroso, R. L., "Filaments in the Sheath Evolution of the Dense Plasma Focus as Applied to Intense Auroral Observations," *IEEE Transactions on Plasma Science*, Vol. 35, No. 4, 2007, p. 808. doi:10.1109/TPS.2007.897483

[31] Feugeas, J., and von Pamel, O., "Current Distribution During the Breakdown in a Coaxial Electrode System," *Journal of Applied Physics*, Vol. 66, No. 3, 1989, pp. 10–80.

[32] Kleev, A. I., and Velikovich, A. L., "Filamentation Instabilities of Dynamic z Pinches and Theta Pinches," *Plasma Physics and Controlled Fusion*, Vol. 32, No. 10, 1990, pp. 7–63.

[33] Shokri, B., Khorashadi, S. M., and Dastmalchi, M., "Ion-Acoustic Filamentation of a Current-Driven Plasma," *Physics of Plasmas*, Vol. 9, No. 8, 2002, pp. 33–55.

R. Myers
Associate Editor